Heterogeneity of Circulating Tumor Cell–Associated Genomic Gains in Breast Cancer and Its Association with the Host Immune Response

Nisha Kanwar[1,2], Zaldy Balde[1,2], Ranju Nair[2], Melanie Dawe[2], Shiyi Chen[3], Manjula Maganti[2], Eshetu G. Atenafu[2], Sabrina Manolescu[1], Carrie Wei[2], Amanda Mao[1], Fred Fu[4], Dan Wang[5], Alison Cheung[5], Yulia Yerofeyeva[5], Rachel Peters[5], Kela Liu[5], Christine Desmedt[6], Christos Sotiriou[6], Borbala Szekely[7], Janina Kulka[7], Trevor D. McKee[4], Naoto Hirano[2,8], John M.S. Bartlett[1,9], Martin J. Yaffe[5,9], Philippe L. Bedard[2], David McCready[2], and Susan J. Done[1,2,10]

ABSTRACT

Tumor cells that preferentially enter circulation include the precursors of metastatic cancer. Previously, we characterized circulating tumor cells (CTC) from patients with breast cancer and identified a signature of genomic regions with recurrent copy-number gains. Through FISH, we now show that these CTC-associated regions are detected within the matched untreated primary tumors of these patients (21% to 69%, median 55.5%, $n = 19$). Furthermore, they are more prevalent in the metastases of patients who died from breast cancer after multiple rounds of treatment (70% to 100%, median 93%, samples $n = 41$). Diversity indices revealed that higher spatial heterogeneity for these regions within primary tumors is associated with increased dissemination and metastasis. An identified subclone with multiple regions gained (MRG clone) was enriched in a posttreatment primary breast carcinoma as well as multiple metastatic tumors and local breast recurrences obtained at autopsy, indicative of a distinct early subclone with the capability to resist multiple lines of treatment and eventually cause death. In addition, multiplex immunofluorescence revealed that tumor heterogeneity is significantly associated with the degree of infiltration of B lymphocytes in triple-negative breast cancer, a subtype with a large immune component. Collectively, these data reveal the functional potential of genetic subclones that comprise heterogeneous primary breast carcinomas and are selected for in CTCs and posttreatment breast cancer metastases. In addition, they uncover a relationship between tumor heterogeneity and host immune response in the tumor microenvironment.

Significance: As breast cancers progress, they become more heterogeneous for multiple regions amplified in circulating tumor cells, and intratumoral spatial heterogeneity is associated with the immune landscape.

Introduction

Intertumor heterogeneity is present in breast cancer on both morphologic and molecular levels. The METABRIC study analyzed somatic mutations, copy-number alterations, and gene expression of 2,509 breast cancers and revealed that they are much more heterogeneous than was previously known, with 10 clinically distinct subtypes (1). Tumor heterogeneity develops along two axes: temporal and spatial. Heterogeneity that occurs within geographically separate areas of the same tumor is termed intratumor or spatial heterogeneity. As the tumor mass expands, its composition at different locations can be quite different (2). This spatial heterogeneity is likely the reason why tumors fail to respond to treatments over time. Targetable aberrations in one part of the tumor are missed when they are not included in diagnostic sampling. Temporal heterogeneity refers to the increasing degree of genetic diversity over time. In breast cancer, this occurs over three transitions: *in situ* carcinoma to invasive breast cancer; evolution of the primary invasive cancer; and progression from primary to metastatic breast cancer (3). Many studies have reported a shift in abundance of a major clone from ductal carcinoma *in situ* to invasive ductal carcinoma, as well as from primary to metastatic cancer (4–9). Circulating tumor cells (CTC) are thought be the earliest detectable cells with metastatic potential; however, CTCs may not be representative of the whole tumor as a result of spatial and temporal heterogeneity. Furthermore, systemic therapy induces a selection pressure on subclonal cell populations that influences tumor progression (10). Tumors after treatment can

[1]Department of Laboratory Medicine and Pathobiology, University of Toronto, Toronto, Canada. [2]Princess Margaret Cancer Centre, University Health Network, Toronto, Canada. [3]The Centre for Applied Genomics, The Hospital for Sick Children, Toronto, Canada. [4]STTARR Innovation Centre, University Health Network, Toronto, Canada. [5]Biomarker Imaging Research Laboratory, Sunnybrook Research Institute, Toronto, Canada. [6]Laboratory for Translational Breast Cancer Research, Department of Oncology, KU Leuven, Leuven, Belgium. [7]2nd Department of Pathology, Semmelweis University, Budapest, Hungary. [8]Department of Immunology, University of Toronto, Toronto, Canada. [9]Ontario Institute for Cancer Research, Toronto, Canada. [10]Laboratory Medicine Program, University Health Network, Toronto, Canada.

Note: Supplementary data for this article are available at Cancer Research Online (http://cancerres.aacrjournals.org/).

N. Kanwar and Z. Balde contributed equally to this article.

Corresponding Author: Susan J. Done, Princess Margaret Cancer Centre, University Health Network, 610 University Avenue, Toronto, Ontario M5G 2M9, Canada. Phone: 416-340-4800, ext. 5573; E-mail: susan.done@uhn.ca

Cancer Res 2021;81:6196–206

doi: 10.1158/0008-5472.CAN-21-1079

be significantly different in composition and behavior compared with the original diagnostic sample (11, 12).

Triple-negative breast cancer (TNBC, negative for expression of estrogen, progesterone, and HER2 receptors) is one of the most aggressive subtypes with metastases frequently observed at the time of diagnosis. TNBC is heterogeneous and can be further divided into multiple subclasses. TNBCs have significant intratumor heterogeneity, high mutational burden, and extensive genomic alterations (13–16). They often have a prominent immune cell infiltrate. Generally, the presence of tumor-infiltrating lymphocytes (TIL) is linked to good survival outcomes, although specific subpopulations have been associated with poor survival because of their ability to suppress the antitumorigenic functions of other TILs (17).

We previously characterized CTCs from patients with breast cancer using high-resolution copy-number profiling (18). We identified a signature of 90 genomic regions that were recurrently gained in CTCs. A majority of the regions were on chromosome 19. Primary breast cancer datasets showed that these regions were rarely gained in bulk extracted samples (3%–4% in The Cancer Genome Atlas database, 3% in METABRIC database; ref. 18). We hypothesized that these subclonal populations may be the ones that preferentially enter circulation, resist treatments and metastasize. Our objective was to identify the proportions of tumor cells with CTC gains in patients' primary tumors and metastases, pre- and post-treatment; and identify driver genes within these regions that may be associated with the metastatic process (**Fig. 1A**). Furthermore, given the importance of intratumor heterogeneity in breast cancer, and the increasing importance of cancer immunotherapy, our second objective was to investigate whether tumor heterogeneity in TNBC (assessed by multispectral FISH and multiplex immunofluorescence) is associated with the degree of TIL infiltration and overall survival. Our results show that cells with CTC gains are indeed detected subclonally in primary breast tumors and are enriched in metastases and posttreatment samples. Furthermore, primary TNBC's with high intratumor heterogeneity for our CTC gene signature are more likely to have an increased infiltration of lymphocytes.

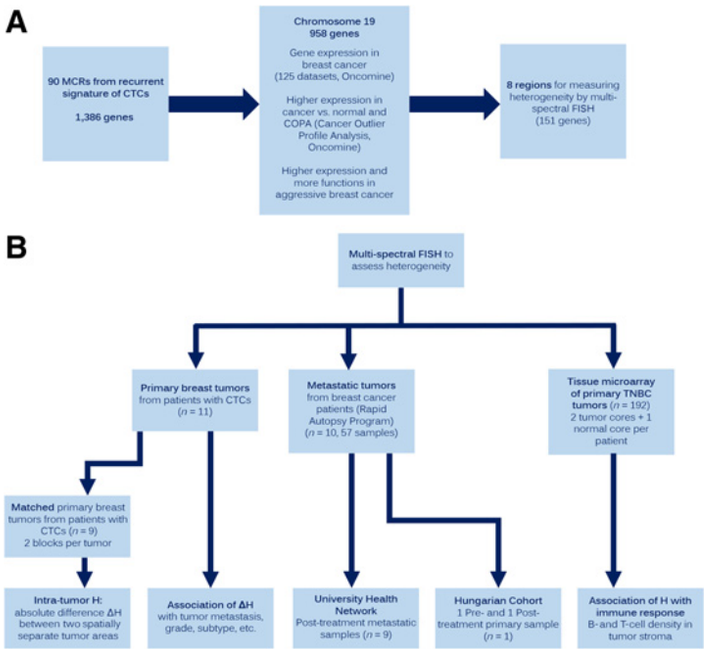

Region Loci (Start-End)	Size (Mb)	Gene Overlapping Probe	Functional Relevance
19p13.3 329975-1540592	1.2	BSG	Induces stromal cells to produce metalloproteinases that aide in invasion; overexpressed in CTCs
19p13.2 8938989-8962178	0.02	MUC16	Upregulated in CTCs with invasive ability
19p13.13 13897508-14127977	0.23	MIR-23-24-27, MIR-181 family	Inhibits apoptosis, therapeutic resistance, evasion of anoikis
19 centromere	0.3	Heterochromatin	Control probe
19q12 30093485-30406322	0.31	CCNE1	Independent prognostic factor in breast cancer (ER-)
19q13.2 3933242-39905317	1.9	TGF-B1	Promoter of EMT, invasion, metastasis
19q13.2 40932895-41305936	0.37	NUMBL	Metastasis and maintenance of tumor initiating cells
19q13.41 45114963-46335814	1.22	KLK family	Early tumor progression, angiogenesis, ECM degradation, invasion
19q13.42 54258550-54657143	0.39	MIR-516, MIR-371-373 family	Clusters co-amplified in embryonic stem cells and cancer, invasion, and metastasis

Figure 1.

Study design and objectives. **A,** Selection of regions/genes from CTC signatures. Using three filtering approaches to select from 90 recurrently gained minimum common regions in CTCs (1,386 genes), we compiled a list of eight regions (151 genes) that may be involved in dissemination of breast cancer cells. The eight regions were assessed using multispectral FISH for intratumoral heterogeneity. **B,** Study objectives. Our goal was to examine the heterogeneity of the eight regions in pretreated matched primary breast tumor samples of 11 patients with CTCs (including 9 patients with two spatially separate tumor samples, which allowed assessment of intratumoral heterogeneity). We also examined 57 posttreated metastatic tumor samples from 9 patients who had died of breast cancer (UHN samples) and one patient with pre- and posttreatment primary samples (Hungarian samples). Furthermore, a TMA consisting of 192 sets of tumors from patients with TNBC was investigated to assess the association of heterogeneity with immune response in this cohort. **C,** Validation of multispectral FISH to measure intratumor heterogeneity. Probes labeled with five nonoverlapping fluorescent spectra were designed to bind across several loci on the p and q arms of chromosome 19. Normal metaphase chromosomes show unique hybridization sites of each probe. Single interphase nuclei may be scored for FISH signals from all five probes simultaneously to measure intratumor heterogeneity of copy-number gains within five chromosomal regions. Using this approach, the eight regions listed were examined for H within primary and metastatic tumors (4 regions + chromosome 19 centromere control per each of two tumor sections). Results used for final analysis included six regions (*TGFB1, KLK10, MUC16, CCNE1, BSG*, and chromosome 19 centromere).

Materials and Methods

Patient tumor samples

Study populations are outlined in detail in **Fig. 1B** and Supplementary Table S1. Patient tumor samples included in this study were from women seen at the Princess Margaret Cancer Centre, Toronto, Canada (except for the Hungarian patient). Primary tumors were from 15 patients recruited for a previous study involving genomic profiling of CTCs. From these, 11 patients had at least a single tumor block for FISH analysis, and 9 patients had two geographically separate tumor blocks for analysis, giving 20 pretreatment primary tumors. Metastatic tumors were from a series of 9 patients who were part of the Rapid Autopsy Program at the University Health Network, Toronto, Canada (UHN cohort- 9 patients, 57 samples posttreatment recurrent or metastatic) and the Breast Cancer Translational Research Laboratory, Institut Jules Bordet, at the Universite Libre de Bruxelles, Brussels, Belgium (Hungarian cohort- 1 patient, 2 samples pre- and posttreatment primary tumor). All patients provided informed consent for prospectively collected samples. All samples were used as per the institutional ethics committee approvals. In the TNBC study, a total of 192 treatment-naïve primary tumors were included. All these patients had surgery followed by adjuvant chemotherapy (according to standardized institutional guidelines).

FISH assay

DNA FISH probes were purchased from Cytocell Ltd (United Kingdom) or from The Center for Applied Genomics facilities, Cytogenomics and Genomics (Toronto, Ontario). BAC clones were selected from the RP-11 library from three overlapping areas for each genomic region of interest using the UCSC Genome Browser (http://genome.ucsc.edu/cgi-bin/hgGateway, Reference Genome: Human Feb.2009 GRCh37/hg19 Assembly). Probes were labeled as per manufacturer's protocols using nick translation (Abbott Molecular) and then precipitated. All protocols for slide preparation, denaturation, hybridization, and washes were followed as per manufacturer's instructions for formalin-fixed paraffin-embedded (FFPE) samples. Five regions of interest were probed simultaneously by preparing a probe mixture of 2 μL per probe for a total of 10 μL of probe: hybridization buffer mixture.

Multispectral fluorescent microscopy

A Zeiss AxioImager Z1 microscope fitted with a Hamamatsu Flash4 camera and Metamorph software was used for imaging. Images for each tumor slide were taken at ×100 magnification consecutively for each of the following filter sets: DAPI, Aqua, FITC, Gold, Texas Red, and Cy5. Each image was captured as a z-stack of 12 slices (∼1 μmol/L per slice). Z-stacks were then collapsed using ImageJ software. Approximately 10 images were captured per tumor sample to ensure at least 100 tumor cells with good-quality probe signals were scored.

FISH scoring and statistical analysis for heterogeneity

A total of 100 cells were scored for each tumor section or core (Supplementary Table S2; ref. 19). To control for tissue thickness, normal tissues were scored and a mean chromosome copy number was obtained for a normal cell for each gene assessed, resulting in thresholds for true single and multiclonal copy gains (Supplementary Table S3). Heterogeneity (H) was measured using the logarithmic Shannon diversity index through the equation $H = \sum - (P_i \times \ln P_i)$, which takes the number of unique cell species (clones) and their proportions within the tumor population into account (20). Briefly, 100 tumor cells were scored for each of the five FISH probes per sample (Supplementary File S1).

Primary samples

The mean ΔH was used as a threshold to obtain two groups with high and low spatial heterogeneity. Fisher exact tests were used to examine the associations between dichotomized ΔH and clinical variables. Bonferroni correction technique was applied to account for the effect of multiple testing.

Metastatic samples

Statistical analyses were completed using SAS 9.4 (SAS Institute Inc.). After pooling the data, we calculated the mean, SD and range of Shannon H in each organ (breast, kidney, liver, and lung). Mean H scores across these organs were compared using ANOVA tests and proportions of high H scores across the organs were compared using χ^2 tests.

Cell line overexpressing single genes and MRG clone genes

293Ta and MCF7 cell lines (ATCC) were maintained in DMEM (+Pen/Strep) supplemented with 10% FBS (Sigma-Aldrich). 293Ta cells were transfected using SBI lentiviral vectors with cDNAs for *BSG, NUMBL, TGFB1, KLK10* and empty control, individually using SBI packaging plasmids and the EndoFectin Lenti Transfection Reagent and kit following manufacturer's protocols. MCF7 cells were transduced with a multiplicity of infection of 2. The clones with multiple genes were generated by sequential transduction with a gap of 1 week. Transduced cells were then selected with puromycin (0.5 μg/mL; Invitrogen) followed by colony picking, and grown individually in a 96-well culture plate. The clones were verified by genomic DNA qPCR to confirm incorporation of cDNA of each single gene and the multiple gene profile (MRG-clone).

In vitro functional assays

Anchorage-independent growth assay

A total of 1,000 cells/well were plated in semisolid medium composed of complete growth medium (CGM), 0.6% noble agar (Difco) over a base composed of 1% noble agar in CGM. Cells were incubated at 37°C with 5% CO_2 for 3 to 4 weeks, and CGM (0.5 mL) was added every 3–4 days. Colonies were counted from 10 fields.

Colony-forming assay

Cells were plated on 24-well tissue culture plates at densities of 200 cells/well. The cells were allowed to adhere to the plates and incubated at 37°C for 14 days, after which, they were fixed and stained with crystal violet. Colonies of 10 or more cells were counted.

Migration assays

Cells were plated at a density of 10,000 cells/well in 0.5 mL in the upper well of 24-well transwell chambers (BD BioCoat Control Inserts, BD Biosciences) with 8.0-μm pore size polycarbonate membrane and 10% FBS DMEM in lower well. After 24 hours at 37°C, 5% CO_2 incubator the cells fixed and stained using the Diff-Quik kit (Dade-Behring). Migration was quantitated by counting cells from five fields.

Each experiment was repeated in triplicate and results averaged.

Measurement of TIL density

A panel of TIL markers was created on the basis of literature review of their functional roles and prognostic values in breast cancer

(Supplementary Table S4). All antibodies have been validated on the platform and experimental protocol was followed (21, 22).

Protein immunofluorescent multiplexing

To assess the density of TILs, protein immunofluorescence multiplexing (MxIF; General Electric Research; ref. 21) was performed (Biomarker Imaging Research Laboratory, Sunnybrook Research Institute, Toronto, Ontario) to detect and score specific lymphocytic subtypes in each tissue microarray (TMA) core. Images were merged to create a composite encompassing all markers for visualizing different cell types and their spatial localizations.

Fluorophore-conjugated antibodies for CD3, CD4, CD8, CD20, FoxP3, PD-L1, and pan-cytokeratin AE1/AE3 were sequentially applied in pairs (Cy3-, Cy5-conjugated) onto a single tissue section, followed by image acquisition and photo-induced chemical bleaching to inactivate optical signals from antibodies (U.S. patent 7,741,045; ref. 23). The tissue section is also labeled with DAPI and imaged during all rounds. Pixel size in this study was 0.293 mm.

Analysis of TILs in MxIF

MxIF images were analyzed to determine the real percentage occupied by TILs for each tissue core. Only the stromal compartment was evaluated (24). Image regions were first classified between intratumor epithelium and stroma by detection of the epithelial pan-cytokeratin marker AE1/AE3. Regions with cytokeratin staining, nonstromal regions (including artifacts or folded tissue), and empty space were excluded from further analysis. An algorithm for cellular and nuclear segmentation was manually optimized for detecting cells based on adjustments of three parameters: nuclear region, membrane region, and expected nuclear size. Fragments were also filtered through another set of features: DAPI nuclear stain intensity, nuclear density, and nuclear size threshold. Solutions were processed across all images for comparative analysis. To test the accuracy of the segmentation, sample regions from each TMA were manually counted using annotation tools in QuPath software and cellular counts were used as the gold standard for determining the solution with automated scores closest to the manual count (24). Manual counts were compared with outputs from the tested segmentation solutions. The selected solution had the following parameter values: nuclear region 0.6, membrane region 2,500, and expected nuclear size of 127.25 μm^2.

The area occupied by TILs and the total stromal area assessed were obtained from Definiens Developer. TIL density was calculated as a percentage by taking the area of each TIL subtype divided by the stromal area assessed for each tumor core as per the International TIL Working Group's recommendations for assessing TILs in breast cancer (25). Because two cores from distant sites of the tumor were taken from each case, a global immune density score was calculated by averaging the two scores.

Ethical approval and consent to participate

Patients provided informed consent to use of prospectively collected samples soon after death. Archival samples used met the requirements for waver of consent as determined by the institutional ethics review board.

Availability of supporting data

All data generated or analyzed during this study are included in this published article (and its Supplementary Data files).

Results

Selection of genomic regions for CTC signature

To prioritize regions of interest, we performed three filtering approaches to select from 90 recurrently gained regions in CTCs, and 1,386 genes within these regions (18). We used the Oncomine gene expression database to select genes that were overexpressed in tumor versus normal tissues from 125 breast cancer datasets with a total of 23,364 cases. We also performed a Cancer Outlier Profile Analysis to select genes that were overexpressed in smaller subsets of tumors (subsets included histologic subtype, nodal involvement, metastasis, reduced survival, increased tumor size, and recurrence). We further selected genes that had higher expression or characterized functions associated with aggressive tumor behavior (cell motility/invasion, intravasation, resistance to anoikis, survival, chemoresistance, and metastasis) based on a review of current literature. We selected eight chromosomal regions (and 151 genes) that may be more strongly associated with dissemination (**Fig. 1A** and **C**). We utilized multispectral FISH to quantify heterogeneity of tumors. Tumors were analyzed to assess the copy number of multiple genomic regions in single cells. Heterogeneity was quantified using the Shannon diversity index (H) that provides a measure of different species at a given location on a logarithmic scale (26). Using this approach, we examined heterogeneity of the eight regions in pretreated matched primary breast tumors of patients from whom CTCs had been previously characterized, and also in posttreated metastatic samples.

Heterogeneity of CTC signature in primary breast cancer

Our objective was to determine the proportion of cells within each tumor with CTC regions gained, and then measure the differences in clonal distribution between the two spatially separate tumor regions from two separate FFPE tumor blocks. We observed vast tumor heterogeneity between patients. Tumors had either high H, where each cell had an observable different profile of CTC gains; or low H, where cells showed more homogeneous CTC gains (**Fig. 2A**). Overall, among all primary tumors, cells with CTC gains were detected in proportions of 5%–18% per clonal species within primary breast tumors, with a range of 21%–69% abnormal cells (average of 57%, median 55.5%) of the total cells analyzed in a tumor.

Spatial heterogeneity was measured in 9 patients as the absolute difference ΔH (H1 − H2) between the two tissue blocks. Cases with low ΔH (5), did not have distant metastasis, regardless of having high H in both blocks (with a corresponding high H_{avg}). However, cases that exhibited high ΔH (4) also had distant metastasis at diagnosis (with a corresponding lower H_{avg}, as a result of each block showing remarkably different H. Therefore, from our results it appears that high spatial heterogeneity (ΔH) was associated with metastasis regardless of the H_{avg} score of the whole tumor (**Fig. 2C**; Supplementary Table S5). Some dominant clones were maintained between blocks of the same patient, new dominant clones also emerged (**Fig. 2B** and **C**).

We compared the composition of species within individual samples with high and low H, and observed that the proportion of tumor cells without CTC gains was higher in low H samples (40.33%) versus high H samples (19.78%) [$P_{adjusted} = 0.0003$; OR = 0.36; 95% confidence interval (CI) = 0.21–0.63]. We also observed that the dominant clones in the low H samples were more likely to be single region gains, compared with the high H samples, which tended to have most or all region gains (Supplementary Table S6A). It is evident that frequent alterations present in CTCs are detectable at subclonal levels (21% to 69% range) in the matched primary tumors, with significant intratumor and intertumor heterogeneity. Overall, higher heterogeneity was

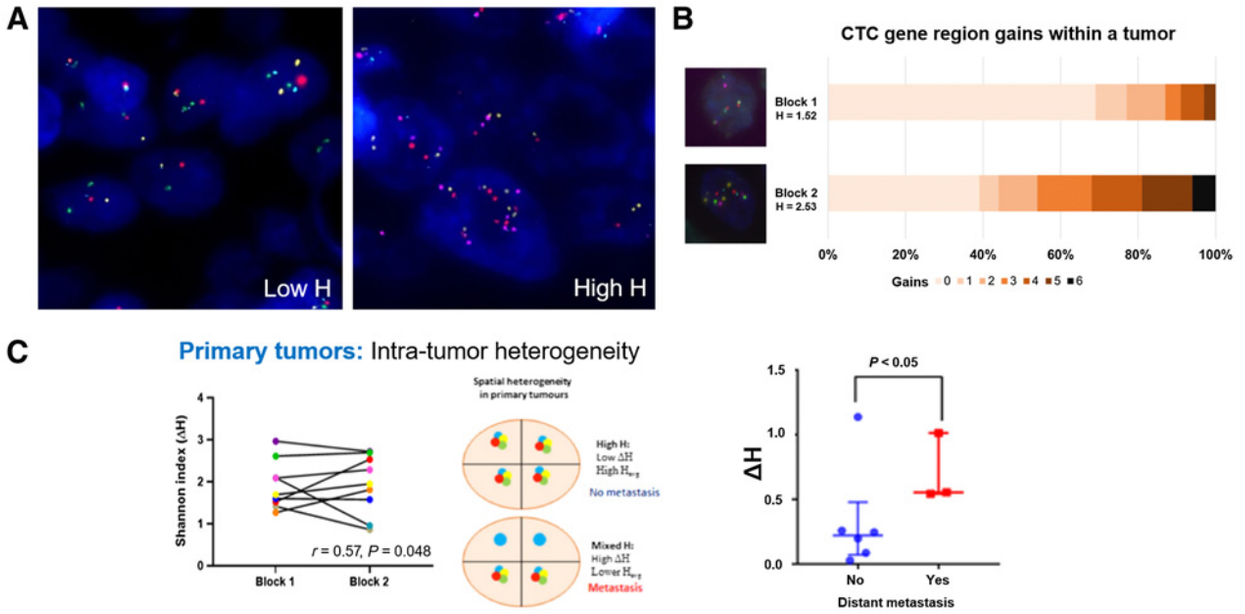

Figure 2.

Increased heterogeneity is associated with metastasis. **A,** Heterogeneity in primary breast tumors. Tumors with low H have the same regions gained in most tumor cells as shown by homogeneity of FISH signals observed in individual tumor cells; tumors with high H have high heterogeneity of the combinations of regions gained for each tumor cell; some tumor cells show single/few FISH signals while other show multiple FISH signals. **B** and **C,** Intratumor or spatial heterogeneity in primary breast tumors. Two spatially separate areas of a tumor were assessed for H in 9 patients. Overall, the correlation coefficient for spatial heterogeneity was found to be moderate ($r = 0.57$, $P = 0.048$); however, it was quite striking in some patients. As an example, Patient 8 exhibits high intratumor or spatial heterogeneity between the two geographically separated tumor blocks, Block 1, H1 = 1.52 and Block 2, H2 = 2.53 (ΔH = 1.01). **C,** Association of ΔH and metastasis of primary breast tumors. Higher intratumor or spatial heterogeneity is associated with distant metastasis regardless of high average H (H_{avg}) of the tumor.

associated with more complex genomic profiles with multiple regions gained (MRG).

Heterogeneity of CTC signature in metastatic breast cancer

We analyzed the heterogeneity of CTC regions in 41 metastatic samples from 8 patients with breast cancer in the UHN cohort. Each patient had between 3–5 metastatic tumors in various organ sites such as breast, lung, liver, kidney, lymph node, and bone. Interestingly, the more regions we included in the CTC signature for H measurements, the higher the heterogeneity result obtained, suggesting increased genomic instability if more regions were assessed per cell (mean of 6 region H = 2.56, mean of 9 region H = 3.54; $P < 0.0001$). This suggests either that cancers that are more unstable are more capable of seeding more metastatic sites, or that instability continues to progress in metastases.

To build upon our results, we sought to determine whether the CTC gains present at low frequencies in primary tumors were preferentially selected for in metastatic tumors. Notably, the metastatic samples were obtained from patients who had died of metastatic disease, which allowed us to identify specific clones that were present in tumors that resisted multiple lines of treatment and ultimately led to death. There was a clear pattern of genomic instability in metastatic samples, where the proportions of cells with CTC gains was significantly higher than primary tumors (range, 70%–100%, mean = 83%, median 93% in metastatic tumors versus range 21%–69%, mean = 57% median = 55.5% in primary tumors; $P < 0.0001$). We compared the heterogeneity for CTC gains between primary ($n = 21$) versus metastatic samples ($n = 41$), and found that there was no significant difference in H between the two groups (mean H of primary = 2.45, mean H of metastases = 2.56; $P = 0.32$; **Fig. 3A**). The most significant difference was that the proportion of tumor cells with an absence of CTC gains was higher in the primary tumor group (mean 43%) versus the metastatic tumor group (17%; $P_{adjusted} < 0.0001$; OR = 0.29; 95% CI = 0.17–0.51). We also observed that the clones that were more likely to be lost in the metastatic group tended to be single region gains. Conversely, the clones that were more frequent in the metastatic group tended to have most or all regions gained (>4 regions gained or "MRG" "MRG" lone; **Fig. 3A** and **B**). A complete list of clones that were most frequent in each group, is presented in **Table 1**. Notably, some patients exhibited similar clonal composition across multiple metastatic sites, strongly suggestive of fitness and selection of these clones during the metastatic process (**Fig. 3B**). From the Hungarian cohort, we compared one pre- and one posttreatment sample from one patient, to determine whether the MRG clones were also selected for. We indeed observed that the pretreated primary tumor had a low frequency of MRG clones compared with the same tumor posttreatment (**Fig. 3C**). Overall, these results support a more aggressive tumor clone that exists at lower frequencies in primary tumors, preferentially enters circulation, resists treatments and ultimately is enriched for in metastasis.

Some clones showed preference for specific organs, suggesting organ-specific routes for dissemination of tumor cells with these CTC gains (Supplementary Table S6B). Notably, tumors that recurred in the breast, had very high proportions of MRG clones (28%, $n = 9$; **Fig. 4A**). This was in contrast to the range of proportions of species/subclones in distant metastatic sites (1%–15%; **Fig. 4B**) and even in primary breast cancers (5%–18%; **Fig. 4A**).

In metastatic breast cancer, there was a clear trend for selection of cells with CTC gains, starting from lower frequency clones in primary

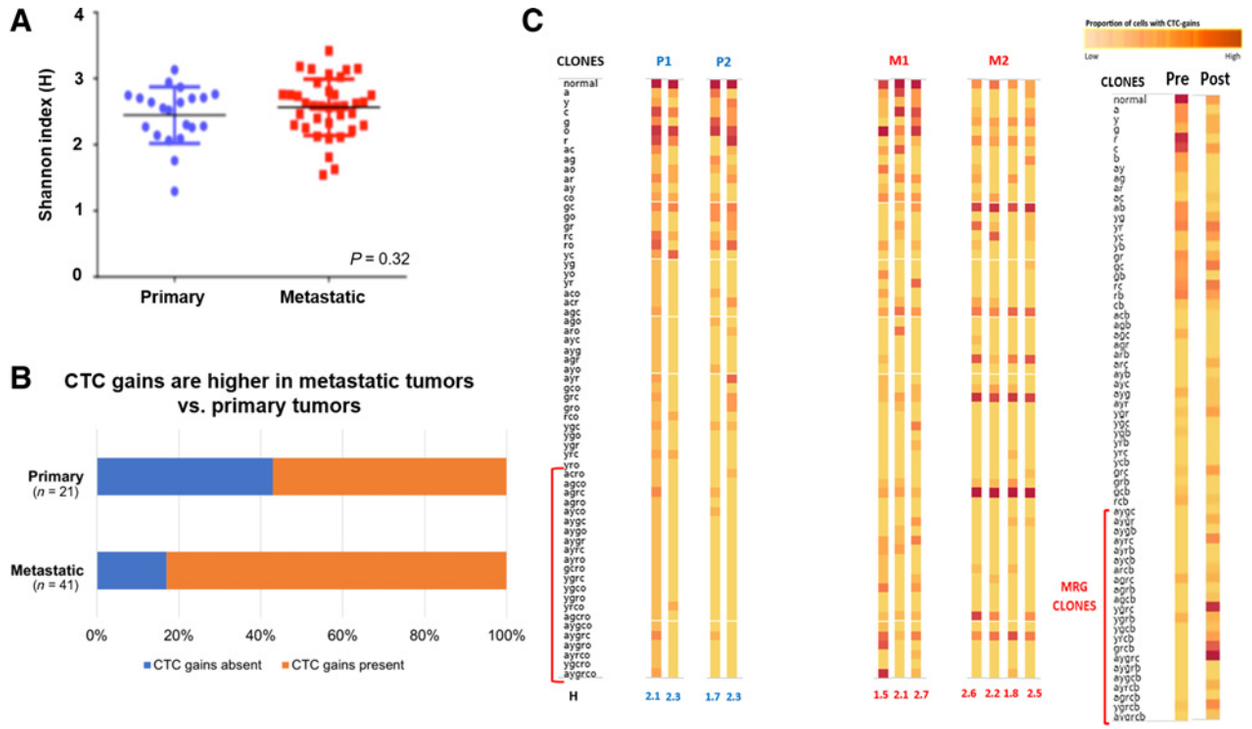

Figure 3.

CTC gains are more frequent in metastatic tumors versus primary tumors. **A,** There was no significant difference in heterogeneity between tumors from primary (n = 19) or metastatic breast cancer (n = 41). **B,** Comparison of clonal composition of primary (n = 19) and metastatic breast tumors (n = 41, UHN cohort). There were significantly higher proportions of cells with CTC gains present in metastatic tumors (mean 83% vs. 57%). Clones with ≥ 4 regions gained (or MRG clones) were observed at higher frequencies in metastatic tumors compared with the primary tumors. Primary tumors were more likely to be comprised of clones with no regions gained or a single region gained. **C,** P1, P2 refer to two primary tumors from two different patients, each with two spatially separate areas. M1, M2 refer to multiple different metastases from the organs of two different patients. There were differences in clonal compositions; primary tumors had larger proportions of clones with single regions gained versus metastatic tumors that had larger proportions of clones with multiple regions gained ("MRG" clones). MRG clones were also present in larger proportions in a posttreatment primary tumor compared with pretreatment, the former showed larger proportions of the MRG clones.

tumors to almost completely making up the metastatic tumors. It is important to note that the degree of H did not change during progression to metastatic disease however, the clonal composition evolved and the proportion of cells without CTC gains drastically diminished. The dominant clones in metastatic tumors, posttreatment primary tumors, and particularly recurrent tumors in the breast, had most or all CTC regions gained.

MRG clones show increased anchorage-independent growth and colony-forming ability *in vitro*

To provide functional evidence of our MRG clone hypothesis, we next tested the *in vitro* behavior of breast cancer cells with and without MRG clone alterations. We established cell lines with stable overexpression of single genes from the CTC regions (*KLK10, NUMBL, TGFB1, BSG*), as well as combinations of all genes together (the MRG clone). Four genes were chosen as this is the minimal number of genes that defined the MRG clone. These genes were chosen because of known functions in aggressive tumors (cell motility/invasion, intravasation, resistance to anoikis, survival, chemoresistance, and metastasis) based on review of current literature; therefore a measurable effect of overexpression was anticipated. However, it is important to note that these genes are within larger CTC regions consisting of several other potential drivers of metastasis. Our results show that breast cancer cells with an MRG clone expression profile have significant increases in anchorage-independent growth, and colony-forming ability (**Fig. 4C**). Tumor cells overexpressing single genes, *NUMBL* and *TGFB1*, showed increased levels of migration ability only.

Primary tumors of TNBC reveal high intratumor heterogeneity through the CTC signature

We then investigated the heterogeneity found within TNBC tumors and its relationship with other clinical features. We assembled a cohort of n = 192 patients diagnosed with TNBC at UHN with survival outcome data available, and collected two cores from spatially separate areas from each tumor to assess the spatial heterogeneity that exists in TNBC (**Fig. 1B**). A total of 105 of the 192 cases in the original cohort were assessable with both cores intact after multispectral FISH and MxIF. The age range is from 27 to 99 years of age; however, the majority (70%) of the study group is within 40 to 69 years. On the basis of clinical cancer staging, most (92.7%) patients have tumors with a size of 50 millimeters or less. High-grade (III) tumors were present in 85%.

The distribution of ΔH-scores based on the 8-gene CTC signature reveals most tumors (68/105) have an ΔH-score equal to or less than 0.50, with very few (14/105) greater than 1.00 (**Fig. 5**). Tumors were divided into high and low intratumor heterogeneity using the median score (ΔHmedian = 0.32). Our results show a significant difference in the spatial H score (ΔH) between the two cohorts (P < 0.001), indicating distinct differences in heterogeneity across primary tumors.

Table 1. Clones with MRG or 4–6 regions gained (*) were selected during tumor progression and compared with clones with single regions gained that were more likely to be found in primary tumors.

Clone	OR	P
No regions gained	0.29 (CI = 0.17–0.51) Primary	0.0001
o	0.35 (CI = 0.21–0.57) Primary	0.0001
r	0.17 (CI = 0.09–0.31) Primary	0.0001
ro	0.20 (CI = 0.08–0.49) Primary	0.0005
ar	0.35 (CI = 0.20–0.64) Primary	0.0007
agrc*	6.89 (CI = 2.72–17.48) Metastatic	0.0001
ygco*	10.06 (CI = 4.17–24.25) Metastatic	0.0001
ygrco*	6.13 (CI = 2.80–13.43) Metastatic	0.0001
aygrco*	4.74 (CI = 1.92–11.69) Metastatic	0.0007

Note: ANOVA test (χ^2) of clones that were more likely to be prevalent in metastatic tumors ($n = 41$) compared with primary tumors ($n = 19$).
Abbreviations: a, 19q13.2; c, 19q12; g, 19 centromere; o, 19p13.3; r, 19q13.41; y, 19p13.2.

Intratumor heterogeneity is positively associated with TIL infiltration in primary TNBC

We developed a panel of TIL markers to assess the degree of immune infiltration in primary TNBC using MxIF (**Fig. 6A**; refs. 21, 22). Relationships among the TIL subsets were assessed and several significant colocalizing populations were identified (**Fig. 6B**). Among them, cytotoxic (Tc) and helper T cells (Th) cells showed the strongest correlation ($R = 0.72$, $P < 0.001$). Other significant correlations include cytotoxic and regulatory T cells (Tr; $R = 0.42$, $P < 0.001$), helper and regulatory T cells ($R = 0.33$, $P < 0.001$), and B and helper T cells ($R = 0.24$, $P = 0.012$). In addition, the presence of PD-L1$^+$ cells in the stroma was correlated with helper ($R = 0.24$, $P = 0.012$) and regulatory T cells ($R = 0.33$, $P < 0.001$). Overall, there were prominent colocalizations of specific TIL subtypes, predominantly between subclasses of T lymphocytes.

The Pearson correlation test was used to assess the relationship between ΔH and TIL density for each primary tumor ($n = 105$; **Fig. 6C**). We generated a total TIL density score for the TILs with significant relationships (B and helper T cells). We found a strong positive correlation between total TIL population and intratumor heterogeneity ($R = 0.38$, $P < 0.0001$). B-cell density showed a significant positive correlation with the spatial ΔH scores ($P < 0.001$). Kaplan–Meier survival analysis reveals that B-cell density is significantly associated with good outcome ($P = 0.0004$), with 10-year survival rates of 78% in tumors with high B-cell density (> median 1.22) and 52% in tumors with low B-cell density (Supplementary Fig. S1). Assessed tumors were then grouped by degree of B lymphocytic infiltrate. Survival analysis showed that those in the high infiltrate group had better outcomes compared with those in the low infiltrate group. B-cell density and spatial H-scores of corresponding tumors were then divided into four cohorts based on the combination of high and low ΔH-score and high and low B-cell density. Tumors with a high ΔH and low B-cell density had the worst outcome compared with the other three groups ($P < 0.01$; **Fig. 6D**; Supplementary Table S7). These findings indicate a role for B lymphocytes in predicting the survival outcomes when assessed together with intratumor heterogeneity.

Discussion

Although it is recognized that invasive breast cancers exhibit heterogeneity at a genomic level, the spatial degree and extent has not been well documented (27–30). Consortia such as TCGA and International Cancer Genome Consortium, have data describing bulk or dominant clones, lacking important insights into the subclonal composition of tumors (31). Single-nucleotide sequencing of 50 breast cancer nuclei revealed that the subclonal composition of tumors is underestimated and that no two cancer cells have the same alterations (32). Recent single-cell sequencing studies in breast cancer also revealed that chromosome 19 amplification involving *CCNE1* was not identified from bulk sequencing of the same tumor, and that different copy-number states could be detected in different cell populations (33). Therapeutic resistance may be driven by selection of distinct subclonal alterations. Ideally, both spatial and temporal heterogeneity should be assessed, by sampling multiple regions from single tumors and sampling over time via liquid biopsies, to capture subclonal events that occur during tumor evolution.

We observed that although there was no significant difference in the degree of heterogeneity of CTC signatures between primary and metastatic tumors, there is a clear selection of clones with specific CTC gains with progression to metastasis. The clones exist at low frequencies within primary tumors (mostly between 21%–69%, median 55%), and expand to comprise most of the metastatic tumors (mostly between 70%–100%, median 97%). In addition, the clones have increased genomic imbalances with gain of all measured CTC regions (MRG clones) and these are more likely to dominate the metastases. Breast recurrences harbor these MRG clones at significantly higher proportions than pretreatment primary tumors and metastatic tumors at distant sites. The recurrent cancer in the breast may be more enriched for MRG clones due to preexisting field cancerization alterations (34). Clones with single region gains are either lost during progression as they are not functionally required for future steps, or not selected for dissemination at all. We also showed that tumor cells with the MRG profile indeed show increased survival and colony-forming ability in *vitro* in comparison with tumor cells with single genes overexpressed.

We assessed spatial heterogeneity by measuring ΔH between two geographically separate regions of a tumor. There was high variability between different tumor areas with maintenance of some clones, as well as evolution of new, more complex clones. The larger the ΔH across the tumor, the more likely the tumor was to metastasise. Intratumor or spatial heterogeneity, usually overlooked because of limited sampling, may explain why the number of targetable known drivers for cancers remains low. Although beyond the scope of this study, the long-term association of intratumor heterogeneity with outcome could provide a novel prognostic metric across all cancers. Notably, for the series of cases studied, regardless of high average H across a tumor, if the ΔH was not significantly different between different areas, distant metastasis was not observed.

Even though the MRG clones were not the dominant proportion in primary tumors, they were still present. There are many instances of low-frequency clones that are extremely important therapeutically (35). In breast cancer, although the most frequently mutated genes are *TP53* and *PIK3CA* (>10%), there are numerous driver genes mutated in <3% of tumors that are associated with treatment

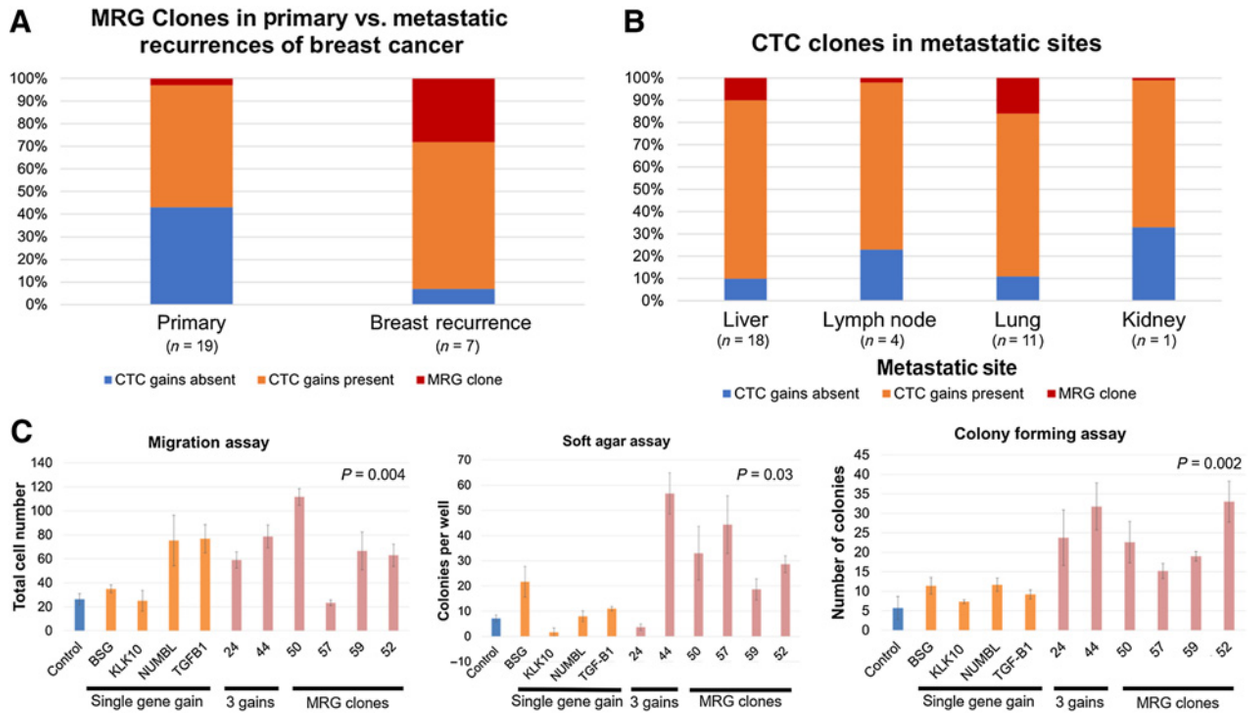

Figure 4.

MRG clones are more frequent in metastatic tumors and increase aggressive tumor behavior. **A,** Significantly smaller proportions of cells with "MRG" clones were detected in primary tumors compared with local breast recurrences and metastatic tumors, suggesting selection of these cells after dissemination and posttreatment. Proportions are presented as averages. **B,** MRG clones were detected in different proportions in distant metastatic sites posttreatment. Primary tumors had smaller proportions of cells with MRG clones compared with local breast recurrences and metastatic tumors in other organs posttreatment. Proportions are presented as averages. **C,** *In vitro* migration, anchorage-independent growth and colony-forming assay validation in stable MCF7 cell lines showed that tumor cells with MRG overexpression profiles increased anchorage independent growth and colony-forming ability than tumor cells with only single genes overexpressed. In contrast, most tumor cell lines showed increased migration ability regardless of their overexpression profile.

resistance (36). In terms of identifying lethal clones, a study in multiple myeloma revealed that a clone that was present in 1% of tumor cells at the time of diagnosis became the dominant clone, and eventually resulted in death (37). In chronic lymphocytic leukemia, in some cases, it is the subclone that holds independent prognostic value for disease progression (38). Investigation of such observations is required to determine synergistic and antagonistic behavior of subclonal events and how they relate to progression and chemoresistance. The issue of clonal cooperation also raises the question of whether it is sufficient to target tumors based on dominant clonal events. Combined anticancer treatment, targeting different drivers or subclonal populations, may be more effective at eradicating the tumor. Ideally, if the cells with metastatic potential could be targeted before they leave the primary tumor, dissemination itself could be blocked.

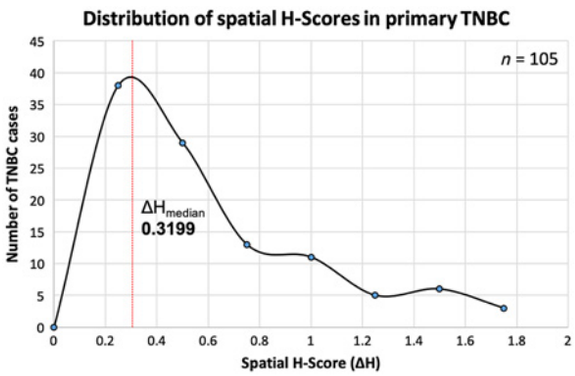

Figure 5.

High intratumor heterogeneity is a relatively rare event in TNBC. Distribution of heterogeneity scores (H-Score) of 105 primary TNBCs using the 8-gene CTC signature. H-scores were calculated using the Shannon diversity index, which uses a logarithmic scale. The majority of patients had a low H-score between 0 and 0.50, with very few over 1.00, resulting in a positive-skew distribution.

Over recent years, there has been increasing interest in characterizing the underlying heterogeneity and immune composition of breast cancers. Few studies have investigated the relationship between these two features in detail, and most research on the immune response has been in other cancer types (39, 40). The high TNBC interpatient variability in spatial H-score (ΔH) is in concordance with previous studies showing a high degree of heterogeneity within TNBCs. Interestingly, we found through survival analyses that high infiltration of B lymphocytes in primary TNBCs was significantly associated with better patient outcomes. The density of $CD20^+$-expressing B lymphocytes was predictive of pCR in a cohort of 108 patients (41, 42). Among all assessed TILs, only $CD20^+$ B and $CD4^+$ Th lymphocytes showed a significant positive relationship with intratumor heterogeneity, with the former having the strongest significance. The positive linear relationship with these TIL subtypes and intratumor heterogeneity suggests that having a highly heterogeneous primary tumor may have a beneficial effect on patient outcome. It is possible that

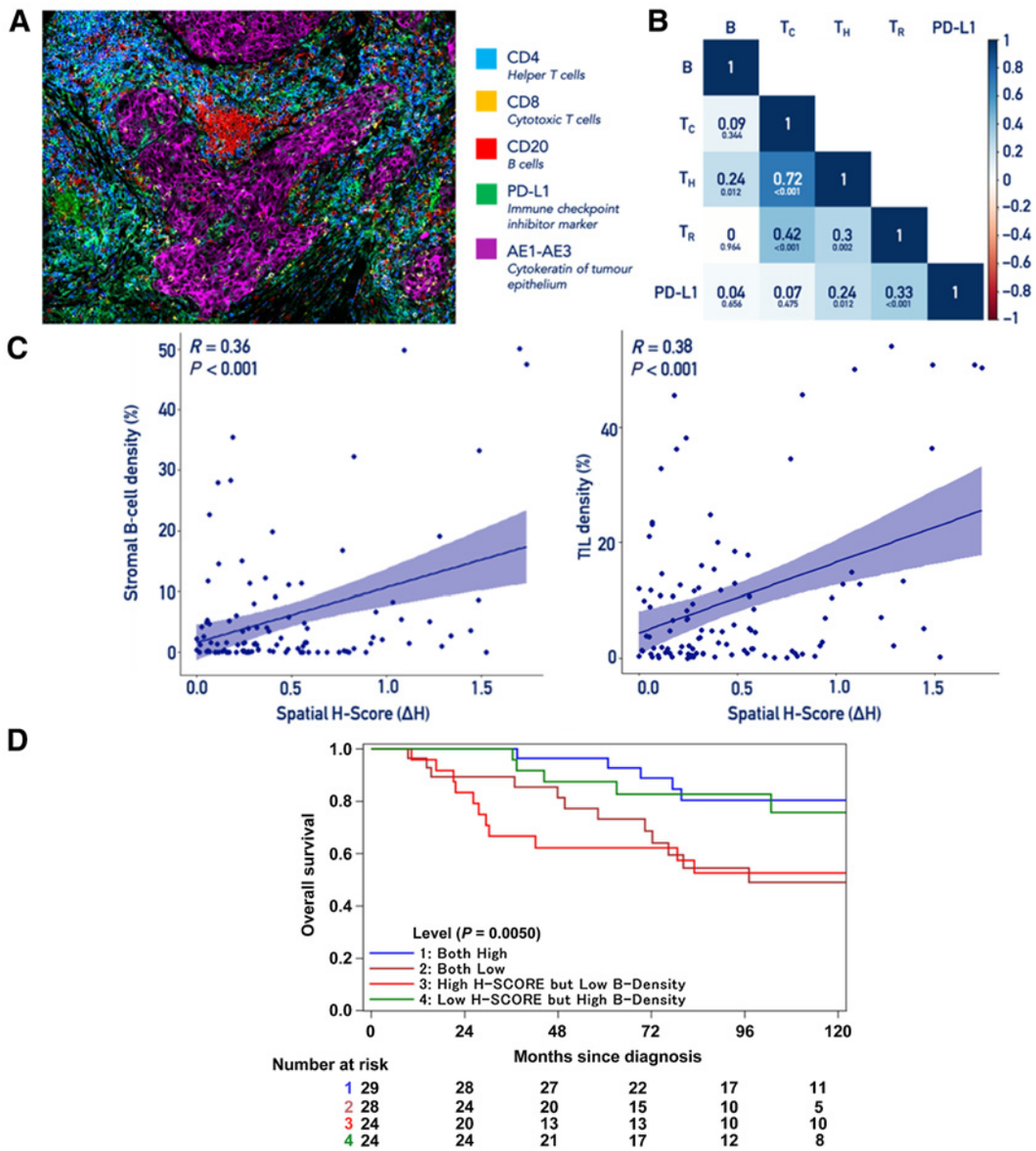

Figure 6.

High intratumor heterogeneity is associated with increased TIL density and improved survival in TNBC patients. **A,** MxIF of primary TNBC tissue cores stained with a panel of antibody markers for each TIL subtype and the tumor epithelium. **B,** Correlation matrix between specific TIL subsets assessed in primary TNBC tumors. Boxes show the degree of correlation between immune markers. B, B-cell density; Tc, cytotoxic T-cell density; Th, helper T-cell density; Tr, regulatory T-cell density; PD-L1^{+}, programmed death ligand 1 positive cell density. The degree of correlation is represented by the color's intensity. The Pearson correlation coefficient (*R*) is indicated in each square, with *P* values below each coefficient. Colocalization was determined through counts of each immune cell across all tumors examined. **C,** Correlation between the H-score and all B lymphocytes or the general TIL population in primary TNBC with *R* and *P* values. Regression line with 95% confidence interval is included. **D,** Kaplan–Meier survival curve of 105 patients with primary TNBCs assessed on the basis of degree of B lymphocyte density and intratumor heterogeneity. Medians for both the B-cell density and the H-score were used to evenly distribute patients into four cohorts of high and low intratumor heterogeneity or B-cell density.

neoantigens in a heterogeneous tumor may increase the ability of TILs to recognize the growing tumors and thus mount a comprehensive adaptive immune response (43). Notably, studies suggest that high levels of TILs in breast cancer are strongly associated with good outcomes (44–50). A highly heterogeneous tumor with a high ΔH score may predict a high degree of immune infiltration. In this way, intratumor heterogeneity may be useful in predicting the likely benefit of immunotherapeutic treatments.

Overall, we have found tumor heterogeneity in both primary and metastatic breast cancer through the CTC signature, and complex genomic profiles with MRG were observed in highly heterogeneous tumors. In addition, tumors with high proportions of MRG clones had increased metastatic activity in multiple cancer cell lines, suggesting a link with tumor heterogeneity and metastatic potential. Furthermore, a high degree of intratumor heterogeneity was observed in primary TNBCs, and was associated with greater infiltration of B lymphocytes,

suggesting a role in the immune response against tumor cells. It should be noted that the analysis of primary and metastatic samples were not from the same patients, so we cannot make definite conclusions about the general selection of MRG clones. However, in the future an accurate measure of heterogeneity may be used to better predict an individual tumor's prognosis and further enhance personalized medicine.

Authors' Disclosures

S.J. Done reports grants from Canadian Institutes of Health Research, Canadian Breast Cancer Foundation—Ontario, Canadian Cancer Society Research Institute; other support from Boutilier Family Triple Negative Breast Cancer Research Fund through the Princess Margaret Cancer Foundation, Ontario Molecular Pathology Research Network, Ontario Ministry of Health and Long Term Care during the conduct of the study. A. Cheung reports grants from Ontario Institute of Cancer Research during the conduct of the study and personal fees from Sunnybrook Research Institute outside the submitted work. C. Sotiriou reports personal fees from Seattle Genetics, Puma, Amgen, Merck & Co. INC., Eisai, Prime Oncology, Exact Sciences; non-financial support from Roche, Genetech, and Pfizer outside the submitted work. T.D. McKee reports personal fees from HistoWiz, Inc. outside the submitted work. N. Hirano reports grants from Takara Bio; personal fees from F. Hoffmann-La Roche, Otsuka Pharmaceutical; and other support from TCRyption outside the submitted work. J.M.S. Bartlett reports personal fees from Insight Genetics, Inc., BioNTech AG, Pfizer, Rna Diagnostics Inc., oncoXchange/MedcomXchange Communications Inc, Herbert Smith French Solicitors, OncoCyte Corporation, Oncology Education; grants, personal fees, and other support from Biotheranostics, Inc., NanoString Technologies, Inc.; personal fees and other support from MedcomXchange Communications Inc.; grants from Thermo Fisher Scientific, Genoptix, Agendia, Stratifyer GmbH; and other support from Breast Cancer Society of Canada outside the submitted work. M.J. Yaffe reports grants from Ontario Institute for Cancer Research during the conduct of the study. P.L. Bedard reports grants from AstraZeneca, Bristol Myers Squibb, Merck, Novartis, GlaxoSmithKline, Amgen, Zymeworks, Bicara, SeaGen, Roche/Genentech, Sanofi, PTC Therapeutics, and Nektar Therapeutics outside the submitted work; and uncompensated advisory for Bristol Myers Squibb, Merck, SeaGen, Amgen, Gilead, Roche/Genentech. No disclosures were reported by the other authors.

Authors' Contributions

S.J. Done: Conceptualization, supervision, funding acquisition, writing–review and editing. **N. Kanwar:** Conceptualization, formal analysis, funding acquisition, validation, investigation, visualization, methodology, writing–original draft, writing–review and editing. **Z. Balde:** Formal analysis, funding acquisition, validation, investigation, visualization, methodology, writing–original draft, writing–review and editing. **R. Nair:** Resources, methodology. **M. Dawe:** Resources, formal analysis, validation, writing–review and editing. **S. Chen:** Formal analysis. **M. Maganti:** Formal analysis. **E.G. Atenafu:** Formal analysis. **S. Manolescu:** Formal analysis, investigation. **C.X. Wei:** Formal analysis, investigation. **A. Mao:** Formal analysis, investigation. **F. Fu:** Software, formal analysis, validation. **D. Wang:** Resources, validation, methodology. **A. Cheung:** Resources, validation, methodology. **Y. Yerofeyeva:** Resources, validation, methodology. **R. Peters:** Resources, validation, methodology. **K. Liu:** Validation. **C. Desmedt:** Resources, formal analysis, investigation, methodology. **C. Sotiriou:** Resources, supervision. **B. Szekely:** Resources, formal analysis, investigation, methodology. **J. Kulka:** Resources, formal analysis, investigation, methodology. **T.D. McKee:** Software, formal analysis, validation, methodology. **N. Hirano:** Supervision, writing–review and editing. **J.M.S. Bartlett:** Supervision, writing–review and editing. **M.J. Yaffe:** Resources, supervision, validation, methodology, writing–review and editing. **P.L. Bedard:** Resources, methodology, writing–review and editing. **D. McCready:** Resources, funding acquisition.

Acknowledgments

The authors thank several groups for providing services for this project, namely James Jonkman from the Advanced Optical Microscopy Facility (AOMF), Andrew Elia for histology services, UHN Biobank, and the Pathology Research Program Laboratory. The authors are grateful to the members of Susan Done's laboratory for their constructive discussions and encouragement throughout the development of this project. They are also deeply appreciative to the patients whose samples were used for this study.

This work was supported by research operating grants from the Canadian Breast Cancer Foundation, Ontario, the Canadian Institute for Health Research, Canadian Cancer Society Research Institute, and the Boutilier Family Triple Negative Breast Cancer Research Fund through the Princess Margaret Cancer Foundation (to S.J. Done). The authors would also like to acknowledge the Canadian Breast Cancer Foundation, Ontario; the Ontario Graduate Scholarship; and the Department of Laboratory Medicine and Pathobiology, University of Toronto for graduate funding support (to Nisha Kanwar and Zaldy Balde). This work also was supported in part by the Ontario Ministry of Health and Long Term Care. The views expressed in this article do not necessarily reflect those of the Ontario Ministry of Health and Long-Term Care.

The costs of publication of this article were defrayed in part by the payment of page charges. This article must therefore be hereby marked *advertisement* in accordance with 18 U.S.C. Section 1734 solely to indicate this fact.

Received April 7, 2021; revised August 10, 2021; accepted October 25, 2021; published first October 28, 2021.

References

1. Curtis C, Shah SP, Chin S-F, Turashvili G, Rueda OM, Dunning MJ, et al. The genomic and transcriptomic architecture of 2,000 breast tumors reveals novel subgroups. Nature 2012;486:346–52.
2. Waclaw B, Bozic I, Pittman ME, Hruban RH, Vogelstein B, Nowak MA. A spatial model predicts that dispersal and cell turnover limit intratumor heterogeneity. Nature 2015;25:261–4.
3. Zardavas D, Irrthum A, Swanton C, Piccart M. Clinical management of breast cancer heterogeneity. Nat Rev Clin Oncol 2015;12:381–94.
4. Rashid-Kolvear F, Pintilie M, Done SJ. Telomere length on chromosome 17q shortens more than global telomere length in the development of breast cancer. Neoplasia 2007;9:265–70.
5. O'Connell P, Pekkel V, Allred DC, Fuqua SAW, Osborne CK, Clark GM. Analysis of loss of heterozygosity in 399 premalignant breast lesions at 15 genetic loci. J Natl Cancer Inst 1998;90:697–703.
6. Radford DM, Phillips NJ, Fair KL, Ritter JH, Holt M, Donis-Keller H. Allelic loss and the progression of breast cancer. Cancer Res 1995;55:5180–3.
7. Radford DM, Fair KL, Phillips NJ, Ritter JH, Steinbrueck T, Holt MS, et al. Allelotyping of ductal carcinoma *in situ* of the breast: deletion of loci on 8p, 13q, 16q, 17p and 17q. Cancer Res 1995;55:3399–405.
8. Heselmeyer-Haddad K, Berroa Garcia LY, Bradley A, Ortiz-Melendez C, Lee W-J, Christensen R, et al. Single-cell genetic analysis of ductal carcinoma *in situ* and invasive breast cancer reveals enormous tumor heterogeneity yet conserved genomic imbalances and gain of MYC during progression. Am J Pathol 2012;181:1807–22.
9. Hernandez L, Wilkerson PM, Lambros MB, Campion-Flora A, Rodrigues DN, Gauthier A, et al. Genomic and mutational profiling of ductal carcinomas in situ and matched adjacent invasive breast cancers reveals intra-tumor genetic heterogeneity and clonal selection. J Pathol 2012;227:42–52.
10. Yates LR, Gerstung M, Knappskog S, Desmedt C, Gundem G, Van Loo P, et al. Subclonal diversification of primary breast cancer revealed by multiregion sequencing. Nat Med 2015;21:751–9.
11. Mroz EA, Rocco JW. The challenges of tumor genetic diversity. Cancer 2017;123:917–27.
12. Caswell-Jin JL, McNamara K, Reiter JG, Sun R, Hu Z, Ma Z, et al. Clonal replacement and heterogeneity in breast tumors treated with neoadjuvant HER2-targeted therapy. Nat Commun 2019;10:657.
13. Peshkin BN, Alabek ML, Isaacs C. BRCA1/2 mutations and triple negative breast cancers. Breast Dis 2010;32:25–33.
14. Huen MSY, Sy SMH, Chen J. BRCA1 and its toolbox for the maintenance of genome integrity. Nat Rev Mol Cell Biol 2010;11:138–48.
15. Carraro DM, Koike Folgueira MAA, Garcia Lisboa BC, Ribeiro Olivieri EH, Vitorino Krepischi AC, de Carvalho AF, et al. Comprehensive analysis of BRCA1, BRCA2 and TP53 germline mutation and tumor characterization: a portrait of early-onset breast cancer in Brazil. PLoS One 2013;8:e57581.

16. Brianese RC, Nakamura KDDM, Almeida FGDSR, Ramalho RF, Barros BDDF, Ferreira ENE, et al. BRCA1 deficiency is a recurrent event in early-onset triple-negative breast cancer: a comprehensive analysis of germline mutations and somatic promoter methylation. Breast Cancer Res Treat 2018;167:803–14.
17. Savas P, Salgado R, Denkert C, Sotiriou C, Darcy PK, Smyth MJ, et al. Clinical relevance of host immunity in breast cancer: from TILs to the clinic. Nat Rev Clin Oncol 2016;13:228–41.
18. Kanwar N, Hu P, Bedard P, Clemons M, McCready D, Done SJ. Identification of genomic signatures in circulating tumor cells from breast cancer. Int J Cancer 2015;137:332–44.
19. Arsham MS, Barch MJ, Lawce HJ, eds. The AGT Cytogenetics Laboratory Manual, Fourth Edition, 717-831. Hoboken, NJ: Wiley-Blackwell, 2017.
20. Magurran AE. Ecological diversity and its measurement. Princeton University Press, 1988.
21. Clarke GM, Zubovits JT, Shaikh KA, Wang D, Dinn SR, Corwin AD, et al. A novel, automated technology for multiplex biomarker imaging and application to breast cancer. Histopathology 2014;64:242–55.
22. Gerdes MJ, Sevinsky CJ, Sood A, Adak S, Bello MO, Bordwell A, et al. Highly multiplexed single-cell analysis of formalin-fixed, paraffin-embedded cancer tissue. Proc Natl Acad Sci U S A 2013;110:11982–7.
23. Larsen M, Sood A, Park C. Sequential analysis of biological samples; 63.
24. Bankhead P, Loughrey MB, Fernández JA, Dombrowski Y, McArt DG, Dunne PD, et al. QuPath: Open source software for digital pathology image analysis. Sci Rep 2017;7:16878.
25. Salgado R, Denkert C, Demaria S, Sirtaine N, Klauschen F, Pruneri G, et al. The evaluation of tumor-infiltrating lymphocytes (TILs) in breast cancer: recommendations by an International TILs Working Group 2014. Ann Oncol 2015;26:259–71.
26. Chung YR, Kim HJ, Kim YA, Chang MS, Hwang K-T, Park SY. Diversity index as a novel prognostic factor in breast cancer. Oncotarget 2017;8:97114–26.
27. Koop S, MacDonald IC, Luzzi K, Schmidt EE, Morris VL, Grattan M, et al. Fate of melanoma cells entering the microcirculation: over 80% survive and extravasate. Cancer Res 1995;55:2520–3.
28. Campbell LL, Polyak K. Breast tumor heterogeneity: cancer stem cells or clonal evolution? Cell Cycle 2007;6:2332–8.
29. Polyak K. Breast cancer: origins and evolution. J Clin Invest 2007;117:3155–63.
30. Shipitsin M, Campbell LL, Argani P, Weremowicz S, Bloushtain-Qimron N, Yao J, et al. Molecular definition of breast tumor heterogeneity. Cancer Cell 2007;11:259–73.
31. Alizadeh AA, Aranda V, Bardelli A, Blanpain C, Bock C, Borowski C, et al. Toward understanding and exploiting tumor heterogeneity. Nat Med 2015;21:846–53.
32. Wang Y, Waters J, Leung ML, Unruh A, Roh W, Shi X, et al. Clonal evolution in breast cancer revealed by single nucleus genome sequencing. Nature 2014;512:155–60.
33. Baslan T, Kendall J, Volyanskyy K, McNamara K, Cox H, D'Italia S, et al. Novel insights into breast cancer copy number genetic heterogeneity revealed by single-cell genome sequencing. Elife 2020;9:e51480.
34. Abdalla M, Tran-Thanh D, Moreno J, Iakovlev V, Nair R, Kanwar N, et al. Mapping genomic and transcriptomic alterations spatially in epithelial cells adjacent to human breast carcinoma. Nat Comm 2017;8:1245.
35. Gerlinger M, Rowan AJ, Horswell S, Larkin J, Endesfelder D, Gronroos E, et al. Intratumor heterogeneity and branched evolution revealed by multiregion sequencing. N Engl J Med 2012;366:883–92.
36. Ng CK, Martelotto LG, Gauthier A, Wen H-C, Piscuoglio S, Lim RS, et al. Intra-tumor genetic heterogeneity and alternative driver genetic alterations in breast cancers with heterogeneous HER2 gene amplification. Genome Biol 2015;16:107.
37. Keats JJ, Chesi M, Egan JB, Garbitt VM, Palmer SE, Braggio E, et al. Clonal competition with alternating dominance in multiple myeloma. Blood 2012;120:1067–76.
38. Landau DA, Carter SL, Stojanov P, McKenna A, Stevenson K, Lawrence MS, et al. Evolution and impact of subclonal mutations in chronic lymphocytic leukemia. Cell 2013;152:714–26.
39. Gao Y, Chen L, Cai G, Xiong X, Wu Y, Ma D, et al. Heterogeneity of immune microenvironment in ovarian cancer and its clinical significance: a retrospective study. Oncoimmunology 2020;9:1760067.
40. Reuben A, Spencer CN, Prieto PA, Gopalakrishnan V, Reddy SM, Miller JP, et al. Genomic and immune heterogeneity are associated with differential responses to therapy in melanoma. NPJ Genom Med 2017;2:10.
41. Shen M, Wang J, Ren X. New insights into tumor-infiltrating B lymphocytes in breast cancer: clinical impacts and regulatory mechanisms. Front Immunol 2018;9:470.
42. Song IH, Heo S-H, Bang WS, Park HS, Park IA, Kim Y-A, et al. Predictive value of tertiary lymphoid structures assessed by high endothelial venule counts in the neoadjuvant setting of triple-negative breast cancer. Cancer Res Treat 2017;49:399–407.
43. Yi M, Qin S, Zhao W, Yu S, Chu Q, Wu K. The role of neoantigen in immune checkpoint blockade therapy. Exp Hematol Oncol 2018;7:28.
44. Chin Y, Janseens J, Vandepitte J, Vandenbrande J, Opdebeek L, Raus J. Phenotypic analysis of tumor-infiltrating lymphocytes from human breast cancer. Anticancer Res 1992;12:1463–6.
45. Loi S, Sirtaine N, Piette F, Salgado R, Viale G, Van Eenoo F, et al. Prognostic and predictive value of tumor-infiltrating lymphocytes in a phase III randomized adjuvant breast cancer trial in node-positive breast cancer comparing the addition of docetaxel to doxorubicin with doxorubicin-based chemotherapy: BIG 02-98. J Clin Oncol 2013;31:860–7.
46. Denkert C, Loibl S, Noske A, Roller M, Müller BM, Komor M, et al. Tumor-associated lymphocytes as an independent predictor of response to neoadjuvant chemotherapy in breast cancer. J Clin Oncol 2010;28:105–13.
47. Dadmarz R, Sgagias MK, Rosenberg SA, Schwartzentruber DJ. CD4+ T lymphocytes infiltrating human breast cancer recognise autologous tumor in an MHC-class-II restricted fashion. Cancer Immunol Immunother 1995;40:1–9.
48. Schmidt M, Böhm D, von Törne C, Steiner E, Puhl A, Pilch H, et al. The humoral immune system has a key prognostic impact in node-negative breast cancer. Cancer Res 2008;68:5405–13.
49. Buisseret L, Garaud S, de Wind A, Van den Eynden G, Boisson A, Solinas C, et al. Tumor-infiltrating lymphocyte composition, organization and PD-1/PD-L1 expression are linked in breast cancer. Oncoimmunology 2016;6:e1257452.
50. Willard-Gallo K, Buisseret L, Garaud S, Gu-Trantien C, de Wind A, Duquenne S, et al. Abstract PD1-3: the significance of tumor infiltrating lymphocyte density, subset composition and organization in breast cancer. Cancer Res 2015;75:PD1–3.